(Preprint) IAA-AAS-DyCoSS3-014

ATTITUDE AND VIBRATION CONTROL FOR A FLEXIBLE SPACECRAFT WITH DOUBLE-GIMBAL VARIABLE-SPEED CONTROL MOMENT GYROS

Takahiro Sasaki*, Takashi Shimomura†, Sam Pullen‡, and Hanspeter Schaub§

This paper focuses on attitude and vibration control of a flexible spacecraft with two parallel double-gimbal variable-speed control moment gyros (DGVSCMGs). First, in this paper, a gain-scheduled (GS) controller for 3-axis attitude control is designed by the post-guaranteed linear matrix inequalities (LMIs) method with $\mathcal{H}_2/\mathcal{H}_\infty$ constraints. Next, an $\mathcal{H}_2/\mathcal{H}_\infty$ controller for vibration control is designed, then to attain both attitude and vibration control at the same time, obtained two controllers are combined while using the dynamic inversion (DI) technique. Finally, the effectiveness of the proposed combined controller is demonstrated through a numerical example.

INTRODUCTION

Both attitude and vibration control of a flexible spacecraft is of great interest in spacecraft applications. Missions of flexible spacecraft often require high speed attitude maneuver and high pointing accuracy and stabilization. However, the oscillations of flexible solar battery paddles or orbit disturbance torque (e.g. aerodynamics, solar pressure, magnetic toque) prevent such mission requirements. Additionally, model uncertainty of the flexible spacecraft inertia is also critical factor to prevent the mission success.

Attitude maneuver dynamics of a flexible spacecraft is described as time varying and nonlinear which affected by orbit disturbance, model uncertainty and modal frequency of the flexible paddles or antennas. To guarantee robustness of them, linear parameter-varying (LPV) control theory[1] is applied to the attitude control problems. Using LPV control theory, the spacecraft dynamics are modeled as an LPV system to avoid difficulties arising from nonlinearities in the dynamics. A gain-scheduled (GS) controller is applied to this model using linear matrix inequalities (LMIs). To solve LMIs simultaneously, a multi-objective GS controller for evaluating both optimality and robustness can be easily designed.[2]

A variety of control problems have been solved via LMIs under common Lyapunov functions.[1,2] Regarding GS control as in,[1] which can be considered for some class of nonlinear systems which

*Graduate Student, Department of Aerospace Engineering, Osaka Prefecture University, 1-1 Gakuen, Naka, Sakai, Osaka 599-8531, Japan, and Visiting Scholar, Department of Aerospace Engineering Science, University of Colorado Boulder, ECNT 321, 431 UCB, CO 80309-0431 USA.

†Professor, Department of Aerospace Engineering, Osaka Prefecture University, 1-1 Gakuen, Naka, Sakai, Osaka 599-8531, Japan.

‡Senior Research Engineer, Department of Aeronautics and Astronautics, Stanford University, Durand Bldg., Room 250 Stanford, CA 94305-4035 USA.

§Alfred T. and Betty E. Look Professor of Engineering, Department of Aerospace Engineering Science, University of Colorado Boulder, ECNT 321, 431 UCB, CO 80309-0431 USA.

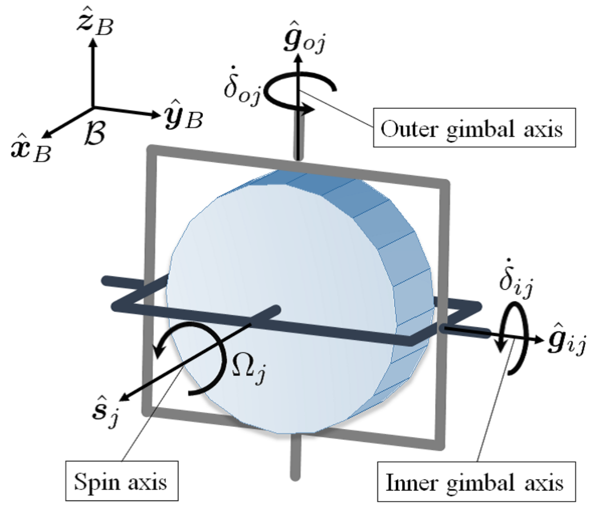

Figure 1. j**-th DGVSCMG.**

can be described as LPV, if one selects a common Lyapunov function for a whole operating range, the overall stability of the closed-loop system as time varying is guaranteed for any changing rate of the scheduling variable. However, selecting a common Lyapunov function for the whole operating range leads to conservatism of design. To avoid such conservatism easily, the post-guaranteed LMI method[3] is proposed, in which the distinct Lyapunov solutions are adopted. This paper adapts this post-guaranteed LMI method to the spacecraft attitude problem and a kind of combined controller for attitude and vibration control is designed while using the dynamic inversion (DI) technique.[6,7]

The attitude actuator considered in this paper is assumed to be a set of two parallel double-gimbal variable-speed control moment gyros (DGVSCMGs)[8,9] to attain high speed attitude maneuver. A DGVSCMG is a new type of multi-degree-of-freedom (multi-DOF) actuator with a lot of advantages. One DGVSCMG can generate three dimensional large torques, which leads to reduction of the number of actuators, the total mass, and volume allocation within the spacecraft. However, a wheel mechanical failure is serious for a DGVSCMG device. Once its wheel has failed, a DGVSCMG is unable to generate any torque. To avoid such situations, it is convenient to introduce redundancy. DGVSCMGs have singularity problem, in which the Jacobian matrix is not calculated . In this paper, a singularity avoidance steering law is proposed, based on singularity robustness (SR) steering with null motion.

EQUATION OF MOTION

In this section, the dynamics of a flexible spacecraft with DGVSCMGs is established and the kinematics with quaternions is described. Then combining both of them, an LPV model for 3-axis attitude control is developed.

Nonlinear dynamics of a Flexible Spacecraft with DGVSCMGs

The spacecraft considered in this paper is assumed to be a flexible body and contains multiple DGVSCMG devices as modeled in Fig. 1. The body-fixed frame $\mathcal{B}$ is represented by a set of unit vectors $\hat{\boldsymbol{x}}_B$, $\hat{\boldsymbol{y}}_B$, and $\hat{\boldsymbol{z}}_B$. The inertial frame is given by $\mathcal{N}$. Symbols $\mathcal{G}_o, \mathcal{G}_i$, and $\mathcal{W}$ denote the outer gimbal axis frame, the inner gimbal axis frame, and the wheel spin axis frame, respectively. Unit vectors $\hat{\boldsymbol{s}}_j$, $\hat{\boldsymbol{g}}_{ij}$, and $\hat{\boldsymbol{g}}_{oj}$ denote spin axis, inner/outer gimbal axis in j-th DGVSCMG, respectively.

Here, the equation of motion (EOM) of a flexible spacecraft with n DGVSCMGs is considered. The total inertial angular momentum $\boldsymbol{H}$ is described by

$$\boldsymbol{H} = \boldsymbol{H}_B + \boldsymbol{H}_{go} + \boldsymbol{H}_{gi} + \boldsymbol{H}_{ws} + \boldsymbol{H}_{\eta} \tag{1}$$

with

$$\boldsymbol{H}_B = [I_s]\boldsymbol{\omega}_{\mathcal{B}/\mathcal{N}} \tag{2a}$$
$$\boldsymbol{H}_{go} = [I_{go}]\boldsymbol{\omega}_{\mathcal{G}_o/\mathcal{N}} \tag{2b}$$
$$\boldsymbol{H}_{gi} = [I_{gi}]\boldsymbol{\omega}_{\mathcal{G}_i/\mathcal{N}} \tag{2c}$$
$$\boldsymbol{H}_{ws} = [I_{ws}]\boldsymbol{\omega}_{\mathcal{W}/\mathcal{N}} \tag{2d}$$
$$\boldsymbol{H}_{\eta} = \boldsymbol{Q}^T\dot{\boldsymbol{\eta}} \tag{2e}$$

where

$$\boldsymbol{\omega}_{\mathcal{G}_o/\mathcal{N}} = \boldsymbol{\omega}_{\mathcal{B}/\mathcal{N}} + \boldsymbol{G}_{go}\dot{\boldsymbol{\delta}}_o \tag{3a}$$
$$\boldsymbol{\omega}_{\mathcal{G}_i/\mathcal{N}} = \boldsymbol{\omega}_{\mathcal{B}/\mathcal{N}} + \boldsymbol{G}_{go}\dot{\boldsymbol{\delta}}_o + \boldsymbol{G}_{gi}\dot{\boldsymbol{\delta}}_i \tag{3b}$$
$$\boldsymbol{\omega}_{\mathcal{W}/\mathcal{N}} = \boldsymbol{\omega}_{\mathcal{B}/\mathcal{N}} + \boldsymbol{G}_{go}\dot{\boldsymbol{\delta}}_o + \boldsymbol{G}_{gi}\dot{\boldsymbol{\delta}}_i + \boldsymbol{G}_{ws}\boldsymbol{\Omega} \tag{3c}$$

and $[I_s]$ is the inertia matrix of a spacecraft excluding DGVSCMG inertia contributions and $\boldsymbol{\omega}_{B/N}$ is the inertial angular velocity of the spacecraft. $[I_{gi}]$ or $[I_{go}]$ is the moment of inertia of the DGVSCMG about the inner or outer gimbal axes, respectively; $[I_{ws}]$ is the moment of inertia of the wheel about the spin axes; and $\boldsymbol{\Omega} = [\Omega_1, \dots, \Omega_n]^T \in R^n$ is the wheel spin rate vector, $\boldsymbol{\delta}_i = [\delta_{i1}, \dots, \delta_{in}]^T \in R^n$ or $\boldsymbol{\delta}_o = [\delta_{o1}, \dots, \delta_{on}]^T \in R^n$ is the inner or outer gimbal angle vector. The matrices of the spin axes, the inner gimbal axes, and the outer gimbal axes are denoted by $\boldsymbol{G}_{ws} = [\hat{\boldsymbol{s}}_1, \dots, \hat{\boldsymbol{s}}_n] \in R^{3\times n}$, $\boldsymbol{G}_{gi} = [\hat{\boldsymbol{g}}_{i1}, \dots, \hat{\boldsymbol{g}}_{in}] \in R^{3\times n}$, and $\boldsymbol{G}_{go} = [\hat{\boldsymbol{g}}_{o1}, \dots, \hat{\boldsymbol{g}}_{on}] \in R^{3\times n}$, respectively. In this flexible model, m elastic modes are considered with $\boldsymbol{\eta} \in R^m$ the modal coordinate vector and $\boldsymbol{Q} \in R^{m\times 3}$ the coupling matrix between flexible and rigid dynamics. The total inertia matrix $[J]$ of a spacecraft including n DGVSCMGs is given by

$$[J] = [I_s] + [I_{go}] + [I_{gi}] + [I_{ws}]. \tag{4}$$

Note that this inertia tensor $[J]$ will vary with time as seen by the body frame. The EOM of a flexible spacecraft follows from the Euler's equation:

$$\dot{\boldsymbol{H}} = \boldsymbol{L}, \tag{5}$$

where the vector $\boldsymbol{L}$ represents the sum of all the external torques experienced by the spacecraft and notation $\boldsymbol{x}^{\times}$ denotes the following skew-symmetric matrix:

$$\boldsymbol{x}^{\times} := \begin{bmatrix} 0 & -x_3 & x_2 \\ x_3 & 0 & -x_1 \\ -x_2 & x_1 & 0 \end{bmatrix}, \ {}^{\forall}\boldsymbol{x} = [x_1\ x_2\ x_3]^T. \tag{6}$$

Substituting Eq. (1) into the LHS in Eq. (5) yields

$$\dot{\boldsymbol{H}}_B + \dot{\boldsymbol{H}}_{go} + \dot{\boldsymbol{H}}_{gi} + \dot{\boldsymbol{H}}_{ws} + \dot{\boldsymbol{H}}_{\eta} = \boldsymbol{L}. \tag{7}$$

In the following development, the short-hand notation $\boldsymbol{\omega} = \boldsymbol{\omega}_{\mathcal{B}/\mathcal{N}}$ is used to make equation description more compact. Similarly, the definitions of the gimbal frame angular velocities and the wheel spin frame angular velocity definitions are shortened such as $\boldsymbol{\omega}_{\mathcal{G}_o/\mathcal{N}} = \boldsymbol{\omega}_{go}$, $\boldsymbol{\omega}_{\mathcal{G}_i/\mathcal{N}} = \boldsymbol{\omega}_{gi}$ and $\boldsymbol{\omega}_{\mathcal{W}/\mathcal{N}} = \boldsymbol{\omega}_{ws}$, respectively. Taking the inertial time derivative of the first term of the LHS in Eq. (7) leads to

$$\dot{\boldsymbol{H}}_B = [I_s]\dot{\boldsymbol{\omega}} + \boldsymbol{\omega}^{\times}[I_s]\boldsymbol{\omega}. \tag{8}$$

The second term of the LHS in Eq. (7) is related to the outer gimbals of the DGVSCMGs. This is shown as follows:

$$\dot{\boldsymbol{H}}_{go} = [I_{go}](\dot{\boldsymbol{\omega}} + \boldsymbol{G}_{go}\ddot{\boldsymbol{\delta}}_o + \boldsymbol{\omega}^{\times}(\boldsymbol{G}_{go}\dot{\boldsymbol{\delta}}_o)) + \boldsymbol{\omega}_{go}^{\times}([I_{go}]\boldsymbol{\omega}_{go}) \tag{9}$$

The third term of the LHS in Eq. (7) is related to the inner gimbals of the DGVSCMGs. This is shown as follows:

$$\dot{\boldsymbol{H}}_{gi} = [I_{gi}](\dot{\boldsymbol{\omega}} + \boldsymbol{G}_{go}\ddot{\boldsymbol{\delta}}_o + \boldsymbol{G}_{gi}\ddot{\boldsymbol{\delta}}_i + \boldsymbol{\omega}^{\times}(\boldsymbol{G}_{go}\dot{\boldsymbol{\delta}}_o + \boldsymbol{G}_{gi}\dot{\boldsymbol{\delta}}_i) + (\boldsymbol{G}_{gi}\dot{\boldsymbol{\delta}}_i)^{\times}(\boldsymbol{G}_{go}\dot{\boldsymbol{\delta}}_o)) + \boldsymbol{\omega}_{gi}^{\times}([I_{gi}]\boldsymbol{\omega}_{gi}) \tag{10}$$

The fourth term of the LHS in Eq. (7) is related to the wheel spin rates of the DGVSCMGs. This is shown as follows:

$$\begin{aligned}\dot{\boldsymbol{H}}_{ws} = [I_{ws}](&\dot{\boldsymbol{\omega}} + \boldsymbol{G}_{go}\ddot{\boldsymbol{\delta}}_o + \boldsymbol{G}_{gi}\ddot{\boldsymbol{\delta}}_i + \boldsymbol{G}_{ws}\dot{\boldsymbol{\Omega}} + \boldsymbol{\omega}^{\times}(\boldsymbol{G}_{go}\dot{\boldsymbol{\delta}}_o + \boldsymbol{G}_{gi}\dot{\boldsymbol{\delta}}_i + \boldsymbol{G}_{ws}\boldsymbol{\Omega}) \\ &+ (\boldsymbol{G}_{go}\dot{\boldsymbol{\delta}}_o)^{\times}(\boldsymbol{G}_{gi}\dot{\boldsymbol{\delta}}_i + \boldsymbol{G}_{ws}\boldsymbol{\Omega}) + (\boldsymbol{G}_{gi}\dot{\boldsymbol{\delta}}_i)^{\times}(\boldsymbol{G}_{ws}\boldsymbol{\Omega})) + \boldsymbol{\omega}_{ws}^{\times}([I_{ws}]\boldsymbol{\omega}_{ws})\end{aligned} \tag{11}$$

The fifth term of the LHS in Eq. (7) is related to the flexible dynamics of a spacecraft. This is shown as follows:

$$\dot{\boldsymbol{H}}_{\eta} = \boldsymbol{Q}^T\ddot{\boldsymbol{\eta}} + \boldsymbol{\omega}^{\times}\boldsymbol{Q}^T\dot{\boldsymbol{\eta}}. \tag{12}$$

In summary, Eq. (7) is rewritten as the final spacecraft/DGVSCMGs kinetic equations of motion:

$$\begin{aligned}[J]\dot{\boldsymbol{\omega}} = &-\boldsymbol{\omega}^{\times}[I_s]\boldsymbol{\omega} - [I_{go}]\boldsymbol{G}_{go}\ddot{\boldsymbol{\delta}}_o - [I_{go}]\boldsymbol{\omega}^{\times}(\boldsymbol{G}_{go}\dot{\boldsymbol{\delta}}_o) - \boldsymbol{\omega}_{go}^{\times}([I_{go}]\boldsymbol{\omega}_{go}) - [I_{gi}]\boldsymbol{G}_{go}\ddot{\boldsymbol{\delta}}_o - [I_{gi}]\boldsymbol{G}_{gi}\ddot{\boldsymbol{\delta}}_i \\ &-[I_{gi}]\boldsymbol{\omega}^{\times}(\boldsymbol{G}_{go}\dot{\boldsymbol{\delta}}_o) - [I_{gi}]\boldsymbol{\omega}^{\times}(\boldsymbol{G}_{gi}\dot{\boldsymbol{\delta}}_i) - [I_{gi}](\boldsymbol{G}_{gi}\dot{\boldsymbol{\delta}}_i)^{\times}(\boldsymbol{G}_{go}\dot{\boldsymbol{\delta}}_o) - \boldsymbol{\omega}_{gi}^{\times}([I_{gi}]\boldsymbol{\omega}_{gi}) - [I_{ws}]\boldsymbol{G}_{go}\ddot{\boldsymbol{\delta}}_o - [I_{ws}]\boldsymbol{G}_{gi}\ddot{\boldsymbol{\delta}}_i \\ &- [I_{ws}]\boldsymbol{G}_{ws}\dot{\boldsymbol{\Omega}} - [I_{ws}]\boldsymbol{\omega}^{\times}(\boldsymbol{G}_{go}\dot{\boldsymbol{\delta}}_o) - [I_{ws}]\boldsymbol{\omega}^{\times}(\boldsymbol{G}_{gi}\dot{\boldsymbol{\delta}}_i) - [I_{ws}]\boldsymbol{\omega}^{\times}(\boldsymbol{G}_{ws}\boldsymbol{\Omega}) - [I_{ws}](\boldsymbol{G}_{go}\dot{\boldsymbol{\delta}}_o)^{\times}(\boldsymbol{G}_{gi}\dot{\boldsymbol{\delta}}_i) \\ &- [I_{ws}](\boldsymbol{G}_{go}\dot{\boldsymbol{\delta}}_o)^{\times}(\boldsymbol{G}_{ws}\boldsymbol{\Omega}) - [I_{ws}](\boldsymbol{G}_{gi}\dot{\boldsymbol{\delta}}_i)^{\times}(\boldsymbol{G}_{ws}\boldsymbol{\Omega}) - \boldsymbol{\omega}_{ws}^{\times}([I_{ws}]\boldsymbol{\omega}_{ws}) - \boldsymbol{Q}^T\ddot{\boldsymbol{\eta}} - \boldsymbol{\omega}^{\times}\boldsymbol{Q}^T\dot{\boldsymbol{\eta}} + \boldsymbol{L}.\end{aligned} \tag{13}$$

The modal equation for a flexible spacecraft can be described as follows:

$$\ddot{\boldsymbol{\eta}} + \boldsymbol{C}\dot{\boldsymbol{\eta}} + \boldsymbol{D}\boldsymbol{\eta} + \boldsymbol{Q}\dot{\boldsymbol{\omega}} = 0, \tag{14}$$

and the damping matrix $\boldsymbol{C}$ and the stiffness matrix $\boldsymbol{D}$ are given by

$$\boldsymbol{C} = \mathrm{diag}\{2\zeta_1\omega_{n1}, \ldots, 2\zeta_1\omega_{nm}\} \tag{15}$$

$$\boldsymbol{D} = \mathrm{diag}\{\omega_{n1}^2, \ldots, \omega_{nm}^2\}. \tag{16}$$

Note that ω_{ni} is the nutural frequency and ζ_i is the modal damping. $(1 \leq i \leq m)$

Kinematics

The quaternion set for attitude descriptions consists of the vector part and the scalar one. Given the principal rotation axis $\hat{\boldsymbol{\alpha}} = [\alpha_x \ \alpha_y \ \alpha_z]^T$ with $\hat{\boldsymbol{\alpha}}^T\hat{\boldsymbol{\alpha}} = 1$ and the rotation angle Θ, the quaternion (Euler Parameters) is (are) defined by

$$\boldsymbol{q} = \begin{bmatrix} \bar{\boldsymbol{q}} \\ q_4 \end{bmatrix} := \begin{bmatrix} \hat{\boldsymbol{\alpha}} \sin \frac{\Theta}{2} \\ \cos \frac{\Theta}{2} \end{bmatrix}, \tag{17}$$

with the constraint:

$$\boldsymbol{q}^T\boldsymbol{q} = \hat{\boldsymbol{\alpha}}^T\hat{\boldsymbol{\alpha}} \sin^2 \frac{\Theta}{2} + \cos^2 \frac{\Theta}{2} = 1. \tag{18}$$

To formulate the attitude tracking problem of a spacecraft, we need the error quaternion $\boldsymbol{q}_e = \boldsymbol{q}_d^{\dagger}\boldsymbol{q}$, where $\boldsymbol{q}$ denotes the current quaternion and $\boldsymbol{q}_d$ denotes the desired quaternion with $\dagger$ meaning the conjugate operation. The kinematics equation is given by

$$\begin{bmatrix} \dot{\bar{\boldsymbol{q}}}_e \\ \dot{q}_{4e} \end{bmatrix} = \frac{1}{2}\boldsymbol{G}(\boldsymbol{q}_e)\boldsymbol{\omega}, \quad \boldsymbol{G}(\boldsymbol{q}_e) := \begin{bmatrix} q_{4e}\boldsymbol{I}_3 + \bar{\boldsymbol{q}}_e^{\times} \\ -\bar{\boldsymbol{q}}_e^T \end{bmatrix}. \tag{19}$$

LPV Model for 3-axis Attitude Control

This paper deals with two parallel DGVSCMGs' allocation depicted as in Fig. 2. In this case, direction matrices in Eq. (13) are given by

$$\boldsymbol{G}_{go} = \begin{bmatrix} 0 & 0 \\ 0 & 0 \\ 1 & 1 \end{bmatrix}, \ \boldsymbol{G}_{gi} = \begin{bmatrix} -\sin\delta_{o1} & -\sin\delta_{o2} \\ \cos\delta_{o1} & \cos\delta_{o2} \\ 0 & 0 \end{bmatrix}, \ \boldsymbol{G}_{ws} = \begin{bmatrix} \cos\delta_{i1}\cos\delta_{o1} & \cos\delta_{i2}\cos\delta_{o2} \\ \cos\delta_{i1}\sin\delta_{o1} & \cos\delta_{i2}\sin\delta_{o2} \\ -\sin\delta_{i1} & -\sin\delta_{i2} \end{bmatrix}. \tag{20}$$

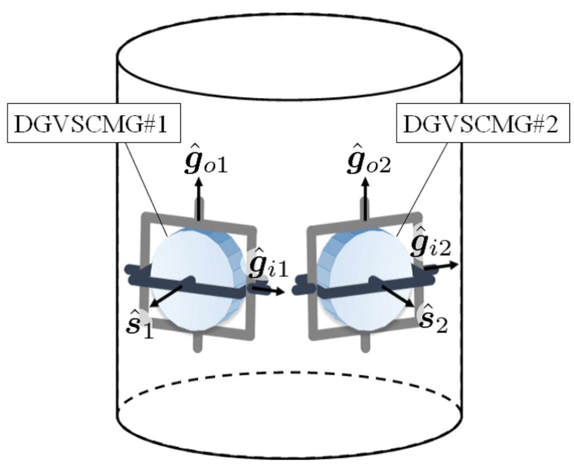

Figure 2. Two parallel DGVSCMGs' allocation.

Here, linear parameter-varying (LPV) model for 3-axis attitude control is introduced. By using Jacobian linearization of Eq. (13) around the equilibrium point ($\boldsymbol{\omega}_{eeq} = \boldsymbol{0}$, $\dot{\boldsymbol{\Omega}}_{eq} = \boldsymbol{0}$, $\dot{\boldsymbol{\delta}}_{ieq} =$

$\mathbf{0}$, $\dot{\boldsymbol{\delta}}_{oeq} = \mathbf{0}$) and the vector part in Eq. (21) around the equilibrium point ($\bar{\boldsymbol{q}}_e = \mathbf{0}$, $\dot{q}_{4e} = 1$), the LPV model of a flexible spacecraft with DGVSCMGs is described as follows:

$$\dot{\boldsymbol{\omega}} = \boldsymbol{A}(\boldsymbol{\rho})\boldsymbol{\omega} + \boldsymbol{B}\boldsymbol{u} + \boldsymbol{E}w \quad (21)$$

$$\bar{\boldsymbol{q}}_e = \frac{1}{2}\boldsymbol{I}_3\boldsymbol{\omega} \quad (22)$$

where

$$\boldsymbol{A}(\boldsymbol{\rho}) = [J]^{-1}[I_{ws}](\boldsymbol{\rho})^{\times}, \quad (23)$$

$$\boldsymbol{B} = -[J]^{-1}[I_{ws}], \quad (24)$$

with

$$\boldsymbol{\rho} = \boldsymbol{G}_s\boldsymbol{\Omega}, \quad (25)$$

$\boldsymbol{E}w$ is disturbance term including the modal terms $\boldsymbol{Q}^T\ddot{\boldsymbol{\eta}}$, $\boldsymbol{\omega}^{\times}\boldsymbol{Q}^T\dot{\boldsymbol{\eta}}$, the orbital disturbance term and the model error such as an uncertainty on the spacecraft inertia matrix $[\boldsymbol{J}]$. The control input $\boldsymbol{u}$ is given as follows:

$$\boldsymbol{u} = \bar{\boldsymbol{B}}\boldsymbol{u}' \quad (26)$$

with

$$\bar{\boldsymbol{B}} = \begin{bmatrix} \boldsymbol{F}_{ws} & \boldsymbol{F}_{gi} & \boldsymbol{F}_{go} \end{bmatrix}, \quad (27)$$

$$\boldsymbol{u}' = \begin{bmatrix} \dot{\boldsymbol{\Omega}} \\ \dot{\boldsymbol{\delta}}_i \\ \dot{\boldsymbol{\delta}}_o \end{bmatrix}, \quad (28)$$

where $\boldsymbol{u}'$ is actuator input vector. This is called steering law of DGVSCMGs. Using this steering law, the DGVSCMGs' system can avoid their singularities. Note that Jacobian matrix $\bar{\boldsymbol{B}}$ is constructed by

$$\boldsymbol{F}_{ws} = \begin{bmatrix} \cos\delta_{i1}\cos\delta_{o1} & \cos\delta_{i2}\cos\delta_{o2} \\ \cos\delta_{i1}\sin\delta_{o1} & \cos\delta_{i2}\sin\delta_{o2} \\ -\sin\delta_{i1} & -\sin\delta_{i2} \end{bmatrix}, \quad \boldsymbol{F}_{gi} = \begin{bmatrix} -\Omega_1\sin\delta_{i1}\cos\delta_{o1} & -\Omega_2\sin\delta_{i2}\cos\delta_{o2} \\ -\Omega_1\sin\delta_{i1}\sin\delta_{o1} & -\Omega_2\sin\delta_{i2}\sin\delta_{o2} \\ -\Omega_1\cos\delta_{i1} & -\Omega_2\cos\delta_{i2} \end{bmatrix},$$
$$\boldsymbol{F}_{go} = \begin{bmatrix} -\Omega_1\cos\delta_{i1}\sin\delta_{o1} & -\Omega_2\cos\delta_{i2}\sin\delta_{o2} \\ \Omega_1\cos\delta_{i1}\cos\delta_{o1} & \Omega_2\cos\delta_{i2}\cos\delta_{o2} \\ 0 & 0 \end{bmatrix}. \quad (29)$$

Note that $\boldsymbol{F}_{ws}$, $\boldsymbol{F}_{gi}$ and $\boldsymbol{F}_{go}$ are torque direction matrix of wheel spin rate, inner gimbal rotation and outer gimbal rotation, respectively.

Combining linearlized dynamics in Eq. (21) and kinematics in Eq. (22), the state-space representation for 3-axis attitude control is given as follows:

$$\begin{bmatrix} \dot{\boldsymbol{\omega}} \\ \dot{\bar{\boldsymbol{q}}}_e \end{bmatrix} = \begin{bmatrix} \boldsymbol{A}(\boldsymbol{\rho}) & \mathbf{0} \\ \frac{1}{2}\boldsymbol{I}_3 & \mathbf{0} \end{bmatrix} \begin{bmatrix} \boldsymbol{\omega} \\ \bar{\boldsymbol{q}}_e \end{bmatrix} + \begin{bmatrix} \boldsymbol{B} \\ \mathbf{0} \end{bmatrix} \boldsymbol{u} + \begin{bmatrix} \boldsymbol{E} \\ \mathbf{0} \end{bmatrix} \boldsymbol{w}. \quad (30)$$

Setting the state variable $\boldsymbol{x} := [\boldsymbol{\omega}_e^T \ \bar{\boldsymbol{q}}_e^T]^T$, the state-space representation of Eq. (30) is rewritten as follows:

$$\dot{\boldsymbol{x}} = \boldsymbol{A}_e(\boldsymbol{\rho})\boldsymbol{x} + \boldsymbol{B}_e\boldsymbol{u} + \boldsymbol{E}_e\boldsymbol{w}. \tag{31}$$

The Jacobian matrices are defined as

$$\boldsymbol{A}_e(\boldsymbol{\rho}) := \begin{bmatrix} \boldsymbol{A}(\boldsymbol{\rho}) & 0 \\ \frac{1}{2}\boldsymbol{I}_3 & 0 \end{bmatrix}, \quad \boldsymbol{B}_e := \begin{bmatrix} \boldsymbol{B} \\ 0 \end{bmatrix}, \quad \boldsymbol{E}_e := \begin{bmatrix} \boldsymbol{E} \\ 0 \end{bmatrix}. \tag{32}$$

CONTROLLER SYNTHESIS

First in this section, attitude controller for 3-axis attitude control is obtained by LPV control theory. Then, attitude and vibration controller is designed while using dynamic inversion (DI).

Gain-Scheduled Attitude Controller

Optimal Gain-Scheduled Controller for 3-axis attitude control is introduced. The generalized plant for Eq. (31) is defined as follows:

$$\begin{cases} \dot{\boldsymbol{x}} = \boldsymbol{A}_e(\boldsymbol{\rho})\boldsymbol{x} + \boldsymbol{B}_e\boldsymbol{u} + \boldsymbol{E}_e\boldsymbol{w} \\ \boldsymbol{z} = \boldsymbol{C}'\boldsymbol{x} + \boldsymbol{D}'\boldsymbol{u} \end{cases} \tag{33}$$

where the coefficient matrix set $(\boldsymbol{C}', \boldsymbol{D}')$ is normally selected such that they normally satisfy the condition $\boldsymbol{C}'^T\boldsymbol{D}' = \boldsymbol{0}$, $\boldsymbol{D}'^T\boldsymbol{D}' > \boldsymbol{0}$, and where $\boldsymbol{w}$ and $\boldsymbol{z}$ are the disturbance input vector and the performance output vector for the simple LPV model in Eq. (31), respectively. This controller is given by

$$\boldsymbol{u} = -\boldsymbol{K}(\boldsymbol{\rho})\boldsymbol{x}. \tag{34}$$

The LPV system and the GS controller are expressed by the following polytopic representation:

$$\boldsymbol{A}_e(\boldsymbol{\rho}) = \sum_{i=1}^{p} \lambda_i(\boldsymbol{\rho})\boldsymbol{A}_{ei}, \tag{35}$$

$$\boldsymbol{K}(\boldsymbol{\rho}) = \sum_{i=1}^{p} \lambda_i(\boldsymbol{\rho})\boldsymbol{K}_i, \tag{36}$$

$$\lambda_i(\boldsymbol{\rho}) \geq 0, \ \sum_{i=1}^{p} \lambda_i(\boldsymbol{\rho}) = 1, \tag{37}$$

where p denotes the number of vertices, in this case, p is equal to $8\ (= 2^3)$. λ is polytopic coefficient. (see in detail in ape of ref) Let us introduce the following mixed $\mathcal{H}_2/\mathcal{H}_\infty$ LMI problem:[2]

$$\inf_{\boldsymbol{W}_i, \boldsymbol{X}, \boldsymbol{Z}} [\text{Trace } (\boldsymbol{Z})] \quad \text{subject to} \tag{38a}$$

$$\Psi_{H2} > 0, \ \ \Psi'_{H2i} < 0, \tag{38b}$$

$$\Psi_{H\infty i} < 0, \tag{38c}$$

$$\text{for all } 1 \leq i \leq p,$$

where

$$
\begin{aligned}
\Psi_{H2} &= \begin{bmatrix} \boldsymbol{X} & * \\ \boldsymbol{E}_e^T & \boldsymbol{Z} \end{bmatrix}, \\
\Psi'_{H2i} &= \begin{bmatrix} (\boldsymbol{A}_{ei}\boldsymbol{X} - \boldsymbol{B}_e\boldsymbol{W}_i) + (\ \bullet\ )^T & * \\ \boldsymbol{C}'\boldsymbol{X} - \boldsymbol{D}'\boldsymbol{W}_i & -\boldsymbol{I} \end{bmatrix}, \\
\Psi_{H\infty i} &= \begin{bmatrix} (\boldsymbol{A}_{ei}\boldsymbol{X} - \boldsymbol{E}_e\boldsymbol{W}_i) + (\ \bullet\ )^T & \boldsymbol{X}\boldsymbol{C}'^T - \boldsymbol{W}_i\boldsymbol{D}'^T & \boldsymbol{E}_e \\ * & -\gamma\boldsymbol{I} & \boldsymbol{D}' \\ * & * & -\gamma\boldsymbol{I} \end{bmatrix},
\end{aligned}
$$

Eqs. (38a) and (38b) guarantee the $\mathcal{H}_2$ performance and Eq. (38c) gives the $\mathcal{H}_\infty$ constraint. Using the optimal solution sets $\boldsymbol{X},\ \boldsymbol{W}_i$ to the problem of Eqs. (38), the extreme controllers $\boldsymbol{K}_i$ at each vertex of the operation range are given by

$$\boldsymbol{K}_i = \boldsymbol{W}_i\boldsymbol{X}^{-1}, \quad 1 \le i \le p. \tag{39}$$

Then, the GS controller is constructed by substituting Eq. (39) into Eq. (36). Note that the common Lyapunov solution $\boldsymbol{X} > 0$ was used in the past GS controller design and resulted in conservatism. As an alternative, post-guaranteed LMI method[?] is used, in which the distinct Lyapunov solutions $\boldsymbol{X}_i > 0$ are adopted. By using this method, mixed $\mathcal{H}_2/\mathcal{H}_\infty$ LMI problem can be described as follows:

$$
\begin{aligned}
&\inf_{\boldsymbol{W}_i,\boldsymbol{X}_i,\boldsymbol{Z}_i} [\mathrm{Trace}\ (\boldsymbol{Z}_i)] \quad \text{subject to} && \text{(40a)} \\
&\tilde{\Psi}_{H2i} > 0,\ \ \tilde{\Psi}'_{H2i} < 0, && \text{(40b)} \\
&\tilde{\Psi}_{H\infty i} < 0, && \text{(40c)} \\
&\text{for each } 1 \le i \le p,
\end{aligned}
$$

where

$$
\begin{aligned}
\tilde{\Psi}_{H2i} &= \begin{bmatrix} \boldsymbol{X}_i & * \\ \boldsymbol{E}_e^T & \boldsymbol{Z}_i \end{bmatrix} \\
\tilde{\Psi}'_{H2i} &= \begin{bmatrix} (\boldsymbol{A}_{ei}\boldsymbol{X}_i - \boldsymbol{B}_e\boldsymbol{W}_i) + (\ \bullet\ )^T & * \\ \boldsymbol{C}'\boldsymbol{X}_i - \boldsymbol{D}'\boldsymbol{W}_i & -\boldsymbol{I} \end{bmatrix} \\
\tilde{\Psi}_{H\infty i} &= \begin{bmatrix} (\boldsymbol{A}_{ei}\boldsymbol{X}_i - \boldsymbol{E}_e\boldsymbol{W}_i) + (\ \bullet\ )^T & \boldsymbol{X}_i\boldsymbol{C}'^T - \boldsymbol{W}_i\boldsymbol{D}'^T & \boldsymbol{E}_e \\ * & -\gamma\boldsymbol{I} & \boldsymbol{D}' \\ * & * & -\gamma\boldsymbol{I} \end{bmatrix}.
\end{aligned}
$$

Using the optimal solution sets $(\boldsymbol{X}_i, \boldsymbol{W}_i)$ to the problem of Eqs. (40), less conservative extreme controllers can be obtained. The extreme controllers are given by

$$\boldsymbol{K}_i = \boldsymbol{W}_i\boldsymbol{X}_i^{-1}, \quad 1 \le i \le p. \tag{41}$$

By using these extreme controllers, a GS controller is again constructed as in Eq. (36). In order to guarantee overall stability and control performance in a whole operation range, we seek a common Lyapunov solution $\boldsymbol{X}_c > 0$ that satisfies the following LMIs:[?]

$$
\begin{aligned}
&\inf_{\boldsymbol{X}_c,\boldsymbol{Z}} [\mathrm{Trace}\ (\boldsymbol{Z})] \quad \text{subject to} && \text{(42a)} \\
&\bar{\Psi}_{H2c} > 0,\ \ \bar{\Psi}'_{H2i} < 0, && \text{(42b)} \\
&\bar{\Psi}_{H\infty i} < 0, && \text{(42c)} \\
&\text{for all } 1 \le i \le p,
\end{aligned}
$$

where

$$
\begin{aligned}
\bar{\Psi}_{H2c} &= \begin{bmatrix} \boldsymbol{X}_c & * \\ \boldsymbol{E}^T & \boldsymbol{Z} \end{bmatrix}, \\
\bar{\Psi}'_{H2i} &= \begin{bmatrix} (\boldsymbol{A}_{ei} - \boldsymbol{B}_e \boldsymbol{K}_i)\boldsymbol{X}_c + (\ \bullet\ )^T & * \\ (\boldsymbol{C}' - \boldsymbol{D}'\boldsymbol{K}_i)\boldsymbol{X}_c & -\boldsymbol{I} \end{bmatrix}, \\
\bar{\Psi}_{H\infty i} &= \begin{bmatrix} (\boldsymbol{A}_{ei} - \boldsymbol{E}_e \boldsymbol{K}_i)\boldsymbol{X}_c + (\ \bullet\ )^T & \boldsymbol{X}_i \boldsymbol{C}'^T - \boldsymbol{K}_i \boldsymbol{X}_c \boldsymbol{D}'^T & \boldsymbol{E}_e \\ * & -\gamma \boldsymbol{I} & \boldsymbol{D}' \\ * & * & -\gamma \boldsymbol{I} \end{bmatrix}.
\end{aligned}
$$

Attitude and Vibration Controller

To attain attitude and vibration control at the same time, vibration controller is designed. From Eq. (14), the state-space representation for vibration control is given as follows:

$$
\begin{bmatrix} \ddot{\boldsymbol{\eta}} \\ \dot{\boldsymbol{\eta}} \end{bmatrix} = \begin{bmatrix} -\boldsymbol{C} & -\boldsymbol{D} \\ \boldsymbol{I} & \boldsymbol{0} \end{bmatrix} \begin{bmatrix} \dot{\boldsymbol{\eta}} \\ \boldsymbol{\eta} \end{bmatrix} + \begin{bmatrix} \boldsymbol{Q} \\ \boldsymbol{0} \end{bmatrix} \dot{\boldsymbol{\omega}} + \begin{bmatrix} \tilde{\boldsymbol{E}} \\ \boldsymbol{0} \end{bmatrix} \tilde{\boldsymbol{w}} \tag{43}
$$

Setting the state variable $\tilde{\boldsymbol{x}} := [\dot{\boldsymbol{\eta}}^T\ \boldsymbol{\eta}^T]^T$, the state-space representation of Eq. (43) is rewritten as follows:

$$
\dot{\tilde{\boldsymbol{x}}} = \tilde{\boldsymbol{A}}_e \tilde{\boldsymbol{x}} + \tilde{\boldsymbol{B}}_e \dot{\boldsymbol{\omega}} + \tilde{\boldsymbol{E}}_e \tilde{\boldsymbol{w}}. \tag{44}
$$

The Jacobian matrices are defined as

$$
\tilde{\boldsymbol{A}}_e := \begin{bmatrix} -\boldsymbol{C} & -\boldsymbol{D} \\ \boldsymbol{I} & \boldsymbol{0} \end{bmatrix}, \quad \tilde{\boldsymbol{B}}_e := \begin{bmatrix} \boldsymbol{Q} \\ \boldsymbol{0} \end{bmatrix}, \quad \tilde{\boldsymbol{E}}_e := \begin{bmatrix} \tilde{\boldsymbol{E}} \\ \boldsymbol{0} \end{bmatrix}. \tag{45}
$$

The generalized plant for Eq. (43) is defined as follows:

$$
\begin{cases} \dot{\tilde{\boldsymbol{x}}} = \tilde{\boldsymbol{A}}_e \tilde{\boldsymbol{x}} + \tilde{\boldsymbol{B}}_e \dot{\boldsymbol{\omega}} + \tilde{\boldsymbol{E}}_e \tilde{\boldsymbol{w}} \\ \tilde{\boldsymbol{z}} = \tilde{\boldsymbol{C}}' \tilde{\boldsymbol{x}} + \tilde{\boldsymbol{D}}' \dot{\boldsymbol{\omega}} \end{cases} \tag{46}
$$

where the coefficient matrix set $(\tilde{\boldsymbol{C}}', \tilde{\boldsymbol{D}}')$ is normally selected such that they normally satisfy the condition $\tilde{\boldsymbol{C}}'^T \tilde{\boldsymbol{D}}' = \boldsymbol{0}$, $\tilde{\boldsymbol{D}}'^T \tilde{\boldsymbol{D}}' > \boldsymbol{0}$, and where $\tilde{\boldsymbol{w}}$ and $\tilde{\boldsymbol{z}}$ are the disturbance input vector and the performance output vector for the simple LPV model in Eq. (43), respectively. This controller is given by

$$
\dot{\boldsymbol{\omega}} = -\tilde{\boldsymbol{K}} \tilde{\boldsymbol{x}}. \tag{47}
$$

Let us introduce the following mixed $\mathcal{H}_2/\mathcal{H}_\infty$ LMI problem again as follows:

$$
\inf_{\tilde{\boldsymbol{W}}, \tilde{\boldsymbol{X}}, \tilde{\boldsymbol{Z}}} \left[\mathrm{Trace}\ \left(\tilde{\boldsymbol{Z}} \right) \right] \quad \text{subject to} \tag{48a}
$$

$$
\bar{\Psi}_{H2} > 0, \ \ \bar{\Psi}'_{H2} < 0, \tag{48b}
$$

$$
\bar{\Psi}_{H\infty} < 0, \tag{48c}
$$

where

$$
\begin{aligned}
\bar{\Psi}_{H2} &= \begin{bmatrix} \tilde{\boldsymbol{X}} & * \\ \tilde{\boldsymbol{E}}_e^T & \tilde{\boldsymbol{Z}} \end{bmatrix}, \\
\bar{\Psi}'_{H2} &= \begin{bmatrix} (\tilde{\boldsymbol{A}}_e\tilde{\boldsymbol{X}} - \tilde{\boldsymbol{B}}_e\tilde{\boldsymbol{W}}) + (\ \bullet\ )^T & * \\ \tilde{\boldsymbol{C}}'\tilde{\boldsymbol{X}} - \tilde{\boldsymbol{D}}'\tilde{\boldsymbol{W}} & -\boldsymbol{I} \end{bmatrix}, \\
\bar{\Psi}_{H\infty} &= \begin{bmatrix} (\tilde{\boldsymbol{A}}_e\tilde{\boldsymbol{X}} - \tilde{\boldsymbol{E}}_e\tilde{\boldsymbol{W}}) + (\ \bullet\ )^T & \tilde{\boldsymbol{X}}\tilde{\boldsymbol{C}}'^T - \tilde{\boldsymbol{W}}\tilde{\boldsymbol{D}}'^T & \tilde{\boldsymbol{E}}_e \\ * & -\gamma\boldsymbol{I} & \tilde{\boldsymbol{D}}' \\ * & * & -\gamma\boldsymbol{I} \end{bmatrix}.
\end{aligned}
$$

Using the optimal solution sets $\tilde{\boldsymbol{X}},\ \tilde{\boldsymbol{W}}$, the optimal controller $\tilde{\boldsymbol{K}}$ is given by

$$\tilde{\boldsymbol{K}} = \tilde{\boldsymbol{W}}\tilde{\boldsymbol{X}}^{-1}. \tag{49}$$

Note that in Eq. (47), the control input is given by $\dot{\boldsymbol{\omega}}$ which is the differential of the upper part of the state vector in general plant for attitude control in Eq. (30). This parameter is difficult to use as a control input. To avoid this difficulty, dynamic inversion (DI) technique is applied.[6,7] Using the desired $\dot{\boldsymbol{\omega}}_{\mathrm{ref}}$ coming from vibration controller in Eq. (47), the desired control input for vibration control $\boldsymbol{u}_v$ is obtained by the following dynamic inversion system:

$$\boldsymbol{u}_v = \boldsymbol{B}^{-1}(\dot{\boldsymbol{\omega}}_{\mathrm{ref}} - \boldsymbol{A}(\boldsymbol{\rho})\boldsymbol{\omega}). \tag{50}$$

Therefore, combining GS attitude controller in Eq. (34) and vibration controller in Eq. (50), attitude and vibration controller $\tilde{\boldsymbol{u}}$ is described by

$$\tilde{\boldsymbol{u}} = \boldsymbol{u} + \boldsymbol{W}'\boldsymbol{u}_v, \tag{51}$$

where the weighting matrix $\boldsymbol{W}'$ is given by

$$\boldsymbol{W}' = \mathrm{diag}\{g_1, g_2, g_3\}, \quad g_i > 0, \quad 1 \le i \le 3. \tag{52}$$

The controller in Eq. (51) to attain attitude and vibration control at the same time can be rewriten by

$$\tilde{\boldsymbol{u}} = -(\boldsymbol{K}_d(\boldsymbol{\rho}) + \boldsymbol{W}'\boldsymbol{B}^{-1}\boldsymbol{A}(\boldsymbol{\rho}))\boldsymbol{\omega} - \boldsymbol{K}_p(\boldsymbol{\rho})\bar{\boldsymbol{q}}_e - \boldsymbol{W}'\boldsymbol{B}^{-1}(\tilde{\boldsymbol{K}}_p\boldsymbol{\eta} + \tilde{\boldsymbol{K}}_d\dot{\boldsymbol{\eta}}), \tag{53}$$

where

$$\boldsymbol{K}_d(\boldsymbol{\rho}) = \boldsymbol{K}(\boldsymbol{\rho}) \times \begin{bmatrix} \boldsymbol{I}_3 \\ \boldsymbol{0}_{3\times3} \end{bmatrix}, \quad \boldsymbol{K}_p(\boldsymbol{\rho}) = \boldsymbol{K}(\boldsymbol{\rho}) \times \begin{bmatrix} \boldsymbol{0}_{3\times3} \\ \boldsymbol{I}_3 \end{bmatrix} \tag{54}$$

$$\tilde{\boldsymbol{K}}_d = \tilde{\boldsymbol{K}} \times \begin{bmatrix} \boldsymbol{I}_3 \\ \boldsymbol{0}_{3\times3} \end{bmatrix}, \quad \tilde{\boldsymbol{K}}_p = \tilde{\boldsymbol{K}} \times \begin{bmatrix} \boldsymbol{0}_{3\times3} \\ \boldsymbol{I}_3 \end{bmatrix}. \tag{55}$$

STEERING LAW DESIGN

CMGs have singularity problem. In this section, singularity avoidance steering law for a spacecraft with DGVSCMGs is proposed. The steering law considered in this paper is rewriten as follws:

$$\boldsymbol{u} = \bar{\boldsymbol{B}}\boldsymbol{u}'. \tag{56}$$

To obtain the actuator input $\boldsymbol{u}'$, inverse matrix of $\bar{\boldsymbol{B}}$ is considered.

Moore-penrose Steering Law

The general solution of Eq. (56) is given by

$$\boldsymbol{u}' = \bar{\boldsymbol{B}}^{\dagger}\boldsymbol{u}, \tag{57}$$

with

$$\bar{\boldsymbol{B}}^{\dagger} = \bar{\boldsymbol{B}}^{T}(\bar{\boldsymbol{B}}\bar{\boldsymbol{B}}^{T})^{-1}. \tag{58}$$

The steering law, it is called "Moore-Penrose steering law", is often used. However, this steering law can not avoid their singularities.

Singularity Robustness Steering Law

To avoid the singularities, a singularity robustness (SR) steering law[10] is proposed as follows:

$$\boldsymbol{u}' = \bar{\boldsymbol{B}}^{\sharp}\boldsymbol{u}, \tag{59}$$

with

$$\bar{\boldsymbol{B}}^{\sharp} = \bar{\boldsymbol{B}}^{T}[\bar{\boldsymbol{B}}\bar{\boldsymbol{B}}^{T} + \alpha\boldsymbol{I}_3]^{-1}, \tag{60}$$

where α is an SR parameter that is a positive scalar to be properly selected. In this paper, a sigmoid function as an SR parameter is introduced as follows:

$$\alpha = \kappa\frac{1-\exp\left(-\frac{1}{m}\right)}{1+\exp\left(-\frac{1}{m}\right)}, \tag{61}$$

with

$$m = \sqrt{\det(\bar{\boldsymbol{B}}\bar{\boldsymbol{B}}^{T})}, \tag{62}$$

where m is a singularity measurement and κ is a positive scalar. Although it can be calculated control input by using this SR steering law, it is not guaranteed to steer gimbal angles away from their singularity.

SR steering law with null motion

To steer gimbal angles away from their singularities, an SR steering law with null motion coming from a redundancy in a DGVSCMGs' system is proposed. A general solution of an SR steering law includes two terms constructed by the particular solution and the homogeneous solution as follows:

$$\boldsymbol{u}' = \bar{\boldsymbol{B}}^{\sharp}\boldsymbol{u} + \tilde{\boldsymbol{W}}\boldsymbol{N} \tag{63}$$

with

$$\tilde{\boldsymbol{W}} = \mathrm{diag}\{w_1, \ldots, w_6\}, \quad w_i > 0, \quad 1 \le i \le 6, \tag{64}$$

$$\boldsymbol{N} = [\boldsymbol{I}_6 - \bar{\boldsymbol{B}}^{\sharp}\bar{\boldsymbol{B}}]\,\boldsymbol{t}, \quad \boldsymbol{t} \in \mathbf{R^6} \tag{65}$$

where the matrix $\boldsymbol{N}$ is the kernel space of $\bar{\boldsymbol{B}}$ and $\tilde{\boldsymbol{W}}$ is the weighting matrix. When $\boldsymbol{t} \neq 0$, the term $\tilde{\boldsymbol{W}}\boldsymbol{N}$ in Eq. (63) presents null motion of the DGVSCMGs' steering law. To steer gimbal angles toward a preferred configuration, the vector $\boldsymbol{t}$ is determined by

$$\boldsymbol{t} = \bar{\boldsymbol{u}}^* - \bar{\boldsymbol{u}} \tag{66}$$

where $\bar{\boldsymbol{u}} = [\boldsymbol{\Omega}^T \boldsymbol{\delta}_i^T \boldsymbol{\delta}_o^T]^T$ is the actuator parameter set vector. the desired actuator parameter set vector $\bar{\boldsymbol{u}}^*$ is approximately selected to realize a desired configuration. By using this steering law, the control input can be calculated and also the gimbal angles can be steered toward prefer configuration away from singularity. In this paper, this steering law in Eq. (63) with Eqs. (65) and (66) is adapted.

NUMERICAL SIMULATION

This section presents attitude maneuver numerical simulations by using the attitude controller in Eq. (34) and combined attitude and vibration controller in Eq. (53). As an example of a flexible spacecraft, the thermoelectric outer planet spacecraft (TOPS) is considered.[11] The flexible parameters characterizing TOPS are represented by the following coupling matrix $\boldsymbol{Q}$ in $\mathrm{Kg}^{1/2}\mathrm{m}$, damping matrix $\boldsymbol{C}$ and stiffness matrix $\boldsymbol{D}$:

$$\boldsymbol{Q} = \begin{bmatrix} -9.4733 & -15.5877 & 0.0052 \\ -0.5331 & 0.4855 & 18.0140 \\ 0.5519 & 4.5503 & 16.9974 \end{bmatrix} \tag{67}$$

$$\boldsymbol{C} = \begin{bmatrix} 0.0059 & 0 & 0 \\ 0 & 0.0075 & 0 \\ 0 & 0 & 0.0097 \end{bmatrix} \tag{68}$$

$$\boldsymbol{D} = \begin{bmatrix} 0.5476 & 0 & 0 \\ 0 & 0.5625 & 0 \\ 0 & 0 & 0.5776 \end{bmatrix}, \tag{69}$$

with the nutural frequency in rad/s

$$\omega_{n1} = 0.7400,\ \omega_{n2} = 0.7500,\ \omega_{n1} = 0.7600, \tag{70}$$

and the modal dampings

$$\zeta_1 = 0.0040,\ \zeta_2 = 0.0050,\ \zeta_3 = 0.0064 \tag{71}$$

associated to the first 3 natural modes ($m = 3$). Inertia tensor $[J]$ is given by

$$[J] = \begin{bmatrix} 1543.9 & -2.3 & -2.8 \\ -2.3 & 471.6 & -35 \\ -2.8 & -35 & 1713.3 \end{bmatrix}. \tag{72}$$

Initial modal coordinate vector and time derivative of modal coordinate vector is $\boldsymbol{\eta}(0) = [0\,0\,0]^T$, $\dot{\boldsymbol{\eta}}(0) = [0\ 0\ 0]^T$, respectively.

The DGVSCMGs' parameters are given in Table 1. The wheel saturation in DGVSCMG is $\Omega = \pm 500\mathrm{rad/s}$ and the limits of the wheel input is $\Omega = \pm 5\mathrm{rad/s^2}$. the limits of the inner/outer gimbal input is $\dot{\delta} = \pm 1\mathrm{rad/s}$.

Table 1. DGVSCMGs' Parameters

Parameter	Value	Unit ($)
$[I_{ws}]$	$\text{diag}[0.0042\ 0.0042\ 0.0042]$	kgm^2
$[I_{gi}]$	$\text{diag}[0.001\ 0.001\ 0.001]$	kgm^2
$[I_{go}]$	$\text{diag}[0.001\ 0.001\ 0.001]$	kgm^2
$\boldsymbol{\Omega}(0)$	[200 300]	rad/s
$\boldsymbol{\delta}_i(0)$	[0 0]	rad
$\boldsymbol{\delta}_o(0)$	$[\pi/4\ \pi/2]$	rad

The disturbance torque[12] experienced by aerodynamics, solar pressure, magnetic torque, and other environmental factors is assumed by

$$\boldsymbol{L} = \begin{bmatrix} 4 \times 10^{-6} + 2 \times 10^{-6} \sin(nt) \\ 6 \times 10^{-6} + 3 \times 10^{-6} \sin(nt) \\ 3 \times 10^{-6} + 3 \times 10^{-6} \sin(nt) \end{bmatrix} \mathrm{N \cdot m}, \tag{73}$$

where n rev/day denotes the orbital frequency. A near-polar orbital satellite is considered in this simulation[13] in this case, $n = 14.57788549$.

The controller design parameters $\boldsymbol{C}'_e$ and $\boldsymbol{D}'_e$ of the GS controller for 3-axis attitude control in Eq. (34) and the disturbance coefficient matrix $\boldsymbol{E}_e$ are given as follows:

$$\boldsymbol{C}'_e = \begin{bmatrix} 10 \times \boldsymbol{I}_3 & 0_{3\times3} \\ 0_{3\times3} & 2 \times \boldsymbol{I}_3 \\ 0_{3\times3} & 0_{3\times3} \end{bmatrix}, \quad \boldsymbol{D}'_e = \begin{bmatrix} 0_{6\times3} \\ 0.01 \times \boldsymbol{I}_3 \end{bmatrix}, \quad \boldsymbol{E}_e = \begin{bmatrix} \boldsymbol{I}_3 \\ \boldsymbol{0}_{3\times3} \end{bmatrix}, \tag{74}$$

the scheduling parameters are given in $-700 \leq \rho_i \leq 700,\ i = 1,\ 2,\ 3$. The controller design parameters $\tilde{\boldsymbol{C}}'_e$ and $\tilde{\boldsymbol{D}}'_e$ of the vibration controller in Eq. (vib) and the disturbance coefficient matrix $\tilde{\boldsymbol{E}}_e$ are given as follows:

$$\tilde{\boldsymbol{C}}'_e = \begin{bmatrix} \boldsymbol{I}_3 & 0_{3\times3} \\ 0_{3\times3} & \boldsymbol{I}_3 \\ 0_{3\times3} & 0_{3\times3} \end{bmatrix}, \quad \tilde{\boldsymbol{D}}'_e = \begin{bmatrix} 0_{6\times3} \\ \boldsymbol{I}_3 \end{bmatrix}, \quad \tilde{\boldsymbol{E}}_e = \begin{bmatrix} \boldsymbol{I}_3 \\ \boldsymbol{0}_{3\times3} \end{bmatrix}, \tag{75}$$

the weighting matrix of the combined attitude and vibration controller $\boldsymbol{W}$ is given by

$$\boldsymbol{W} = \begin{bmatrix} 0.06 & 0 & 0 \\ 0 & 0.06 & 0 \\ 0 & 0 & 0.06 \end{bmatrix}. \tag{76}$$

Steering law to avoid the singularities in Eq. (63) with Eqs. (65) and (66) is adapted. The design parameter for steering law is as follows:

$$\tilde{\boldsymbol{W}} = \begin{bmatrix} 1 & 0 & 0 & 0 & 0 & 0 \\ 0 & 1 & 0 & 0 & 0 & 0 \\ 0 & 0 & 10 & 0 & 0 & 0 \\ 0 & 0 & 0 & 10 & 0 & 0 \\ 0 & 0 & 0 & 0 & 10 & 0 \\ 0 & 0 & 0 & 0 & 0 & 10 \end{bmatrix}, \quad \kappa = 10, \quad \tilde{\boldsymbol{u}}^* = [250\ 250\ 0\ 0\ 0\ pi/2]^T \tag{77}$$

The initial/desired attitude parameter and angular velocity are given in Table 2. This maneuver[4] corresponds to a rotation as follows:

$$\hat{\boldsymbol{\alpha}} = [-2/\sqrt{14}\ 1/\sqrt{14}\ 3/\sqrt{14}]^T \tag{78}$$

$$\Theta = 8/9\pi \tag{79}$$

in Eq. (17). This maneuver rotates thespacecraft 160° around the principal rotation axis $\hat{\boldsymbol{\alpha}}$. And this simulation also consider the model uncertainty $\Delta[J]$ on the inertia tensor $[J]$. Therefore in the numerical simulation, the inertia tensor $[J]$ is given by $[J] + \Delta[J]$ with $\Delta[J] = 0.2[J]$, since the oscillation of the flexible solar battery paddles or flexible parabolic communication antenna prevent the spacecraft inertia matrix from being known exactly in a practical situation. This inertia matrix variation can heavily affect spacecraft attitude, which invariably presents a challenge to the spacecraft attitude control system.[5]

Table 2. Attitude Simulation Parameters

Parameter	Value	Unit ($)
$\boldsymbol{q}(0)$	$[0\ 0\ 0\ 1]^T$	$-$
$\boldsymbol{q}_d$	$[-0.5264\ \ -0.2632\ 0.7896\ 0.1736]^T$	$-$
$\boldsymbol{\omega}(0)$	$[0.03435353\ 0\ 0]^T$	rad/s
$\boldsymbol{\omega}_d$	$[0\ 0\ 0]^T$	rad/s

Figures 3-6 show the comparison of the simulation results by using two controllers. Black lines and green lines show the simulation result by using the GS attitude controller in Eq. (34) and the combined attitude and vibration controller in Eq. (53), respectively.

Figures 3 and 4 shows the attitude behavior of a flexible spacecraft with DGVSCMGs. The time history of the angular velocity of a spacecraft and attitude parameters (quaternions) are shown in Figs. 3 and 4, respectively. From these figures, the 3-axis attitude control have been completely attained.

Figure 5 shows the modal displacements $\boldsymbol{\eta}$. This figure demonstrates the effectiveness of the proposed combined attitude and vibration controller, since the response of the modal displacements is improved and the maximum amplitude value of the result by proposed controller is less than half of that by the attitude controller. Figure 6 shows controller input results. This figure shows the amount of control input coming from proposed controller is almost the same as attitude controller.

Figures 7-11 show the simulation results of the DGVSCMG motion by using the singularity avoidance steering law in Eq. (63). Figures 9 and 10 show wheel input and gimbal input, respectively. From these figures, DGVSCMG input does not exceed limit by torque limiter. Wheel and gimbal motion in Figs 9 and 10 show that wheel angular velocity and gimbal angles converge to preferred DGVSCMG parameter set $\tilde{\boldsymbol{u}}^*$ and also singularity measurement go away from the singularity statement $m = 0$.

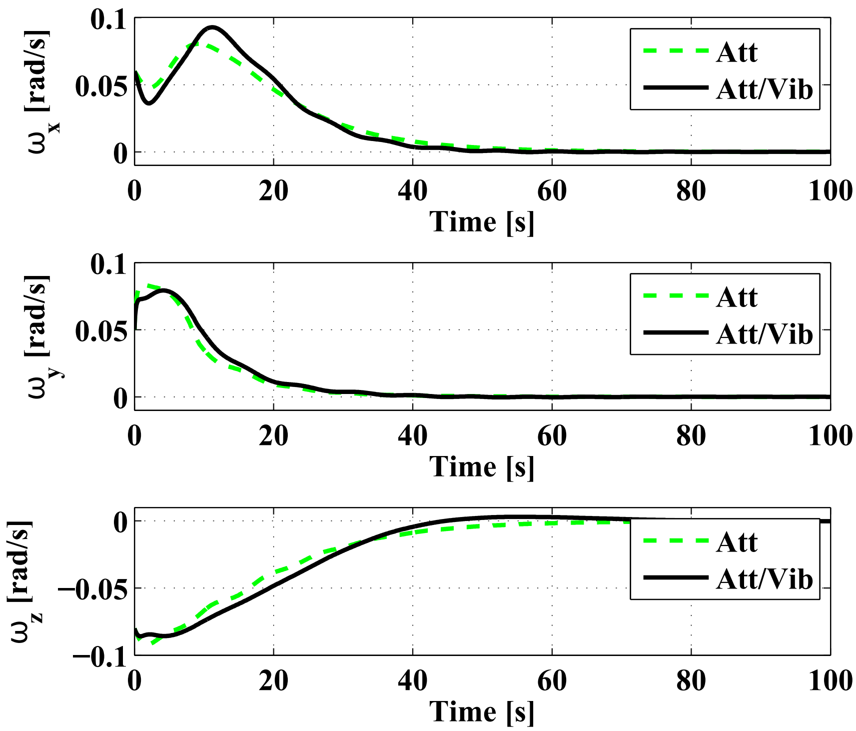

Figure 3. Angular velocity of a spacecraft.

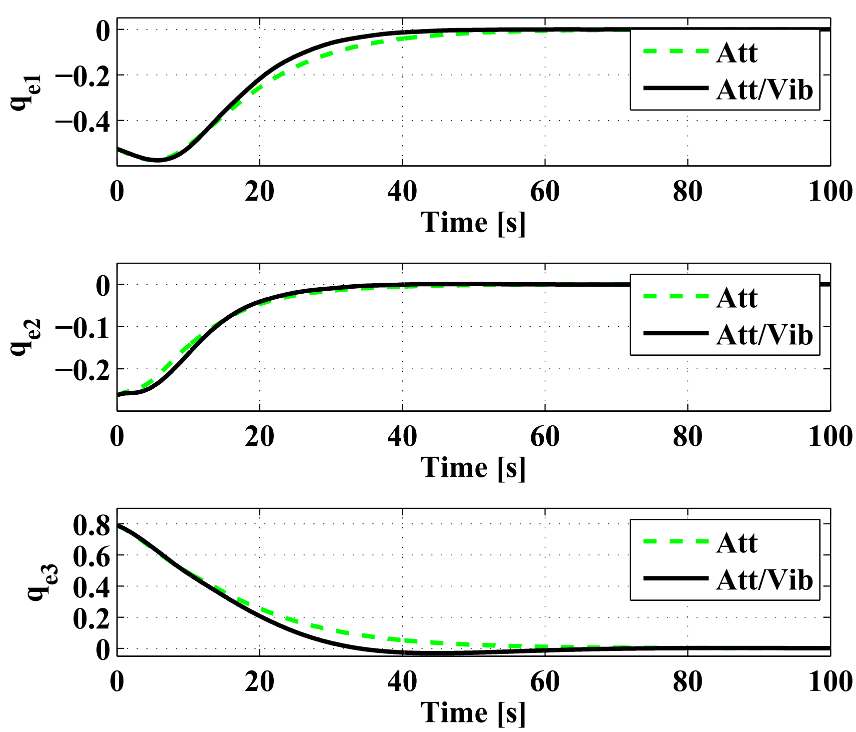

Figure 4. Vector part of quaternion.

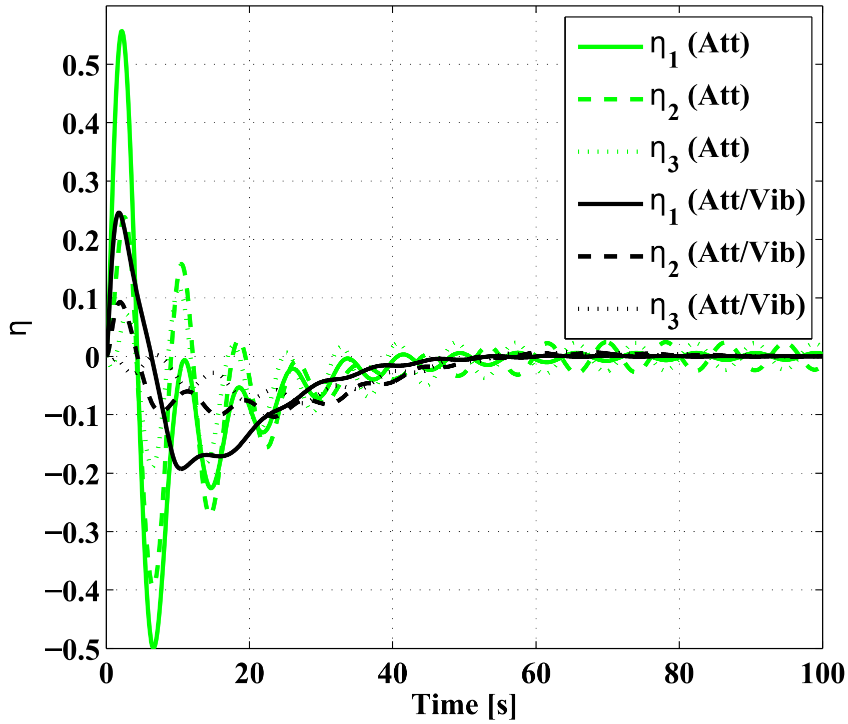

Figure 5. Modal.

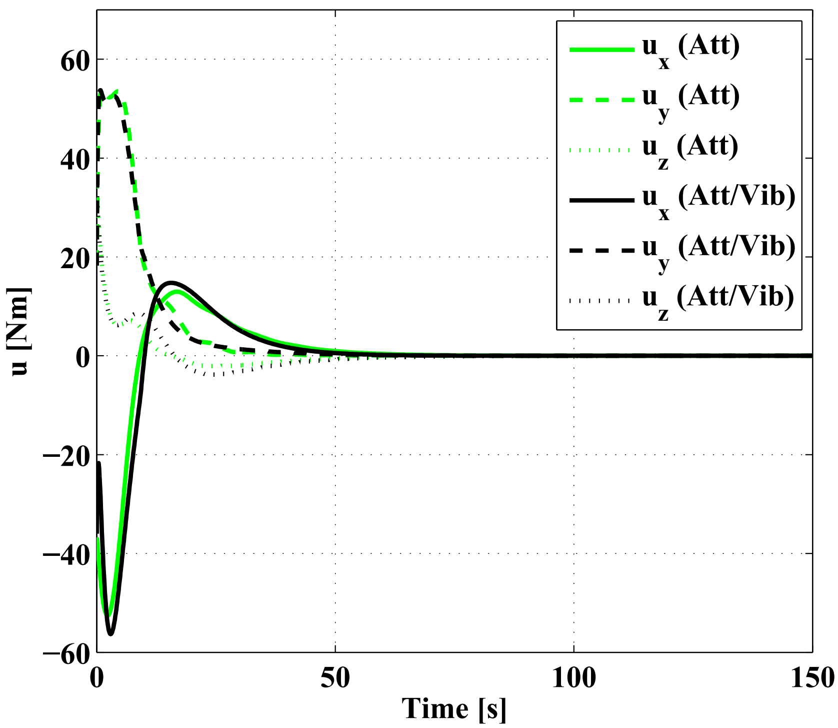

Figure 6. Controller input.

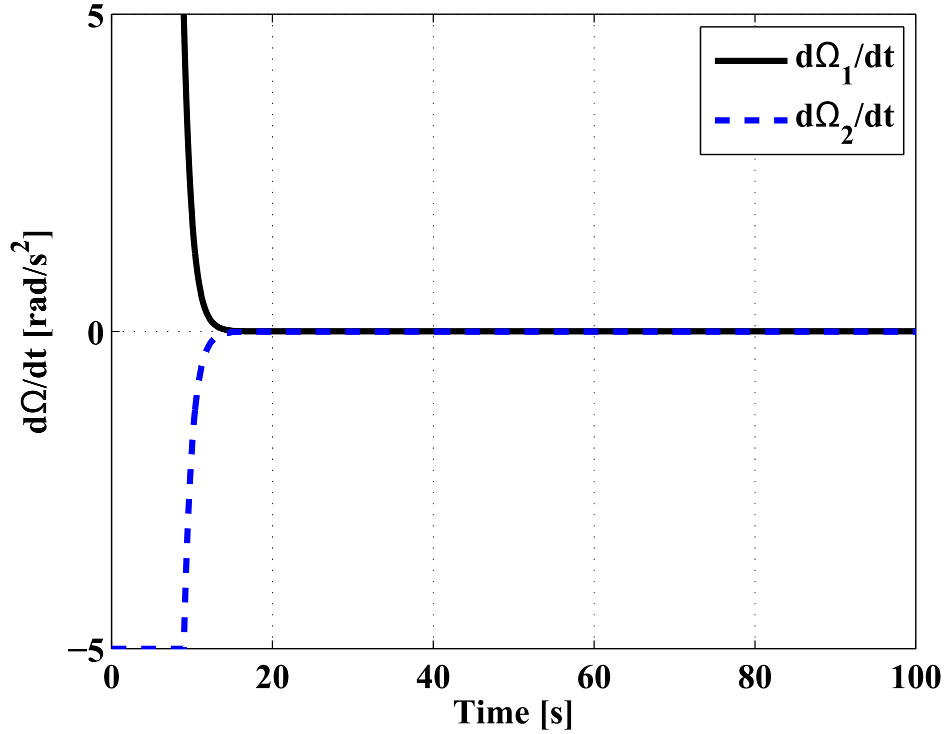

Figure 7. Wheel acceleration (wheel input).

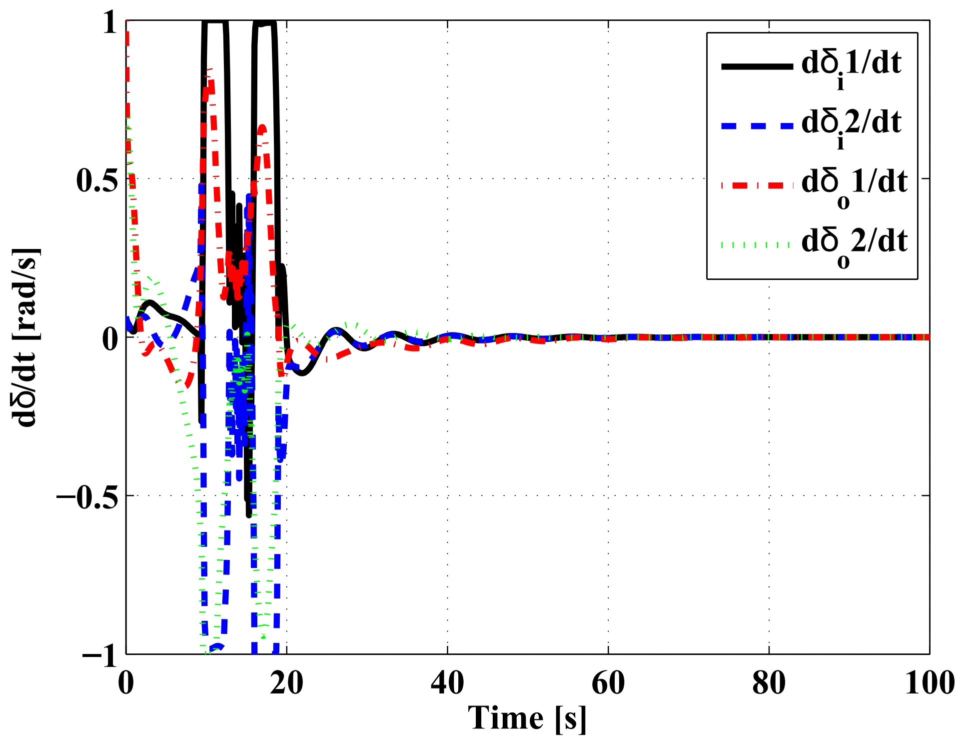

Figure 8. Gimbal angular velocity (gimbal input).

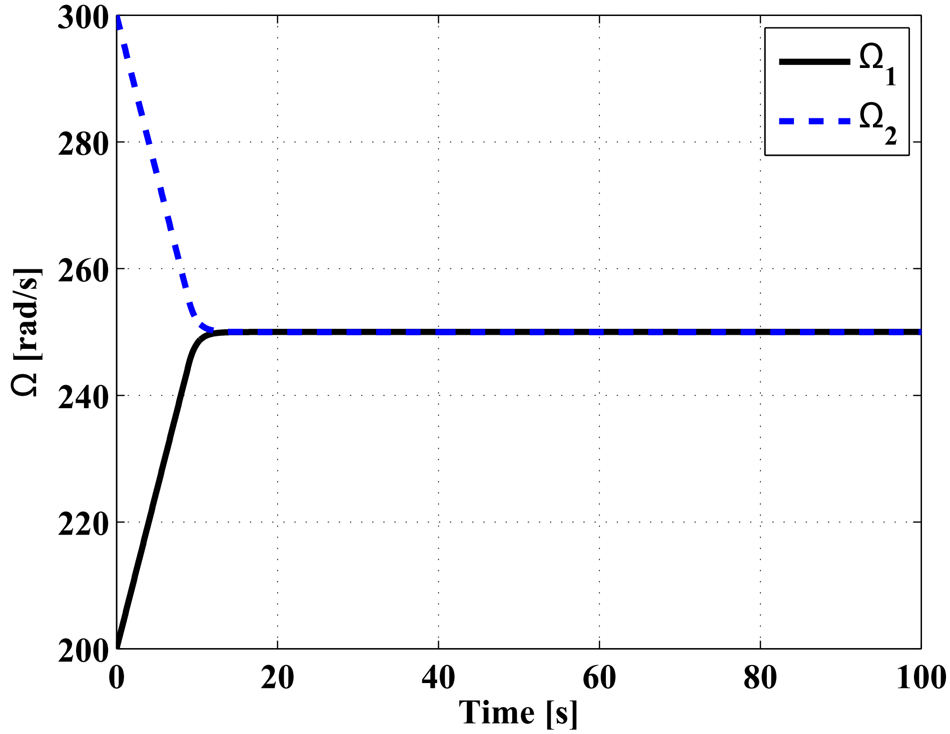

Figure 9. Wheel angular velocity.

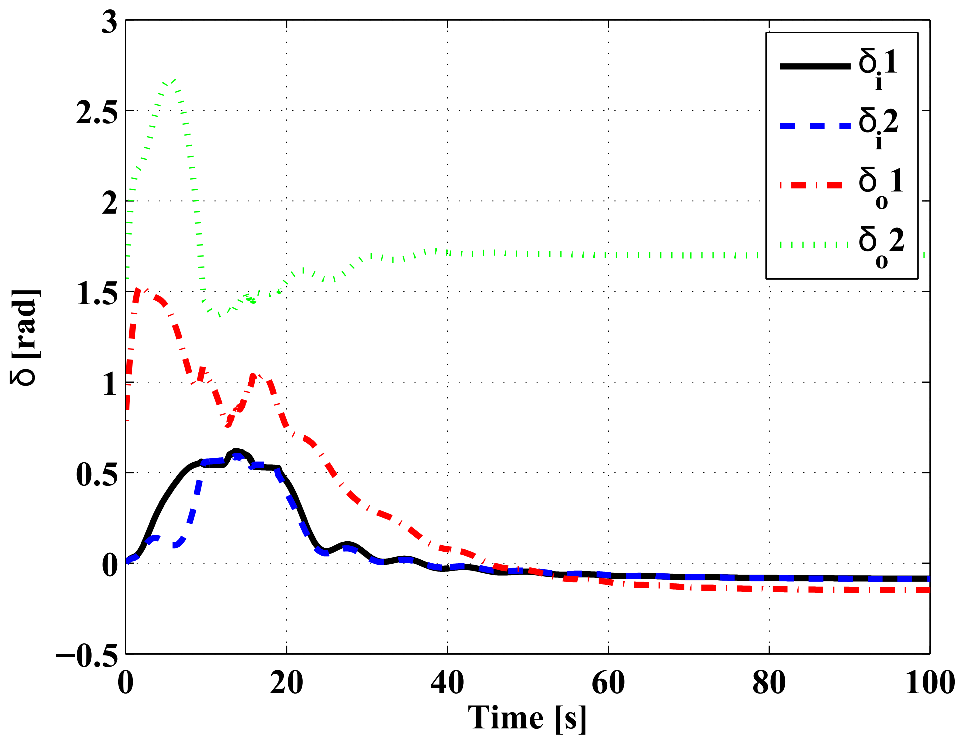

Figure 10. Gimbal angles.

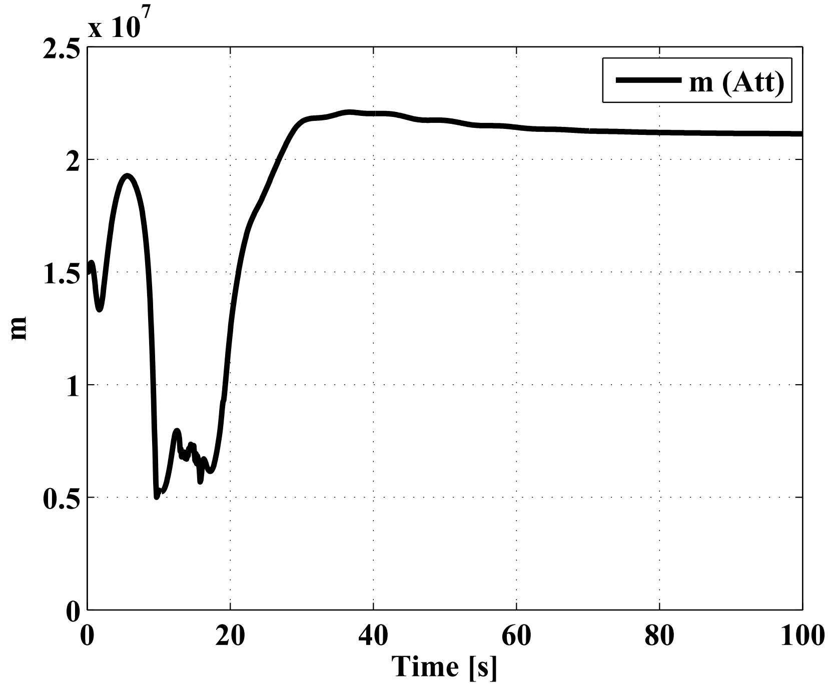

Figure 11. Singularity measurement.

CONCLUSION

In this paper, the dynamics and the linear parameter-varying (LPV) model of a flexible spacecraft equipped with multiple DGVSCMGs has been explored and developed, respectively. Then, a gain-scheduled (GS) controller for 3-axis attitude control has been designed by the post-guaranteed linear matrix inequalities (LMIs) method with $\mathcal{H}_2/\mathcal{H}_\infty$ constraints. Based on the dynamic inversion (DI) technique, a combined controller for attitude and vibration control has been obtained. To avoid the singularity problem of DGVSCMGs, a singularity robustness (SR) steering law with null motion is applied with a sigmoid function as an SR parameter. Finally, the effectiveness of the proposed combined controller and singularity avoidance steering law is demonstrated through a numerical example.

ACKNOWLEDGMENT

This work was supported by JSPS Grant-in-Aid for Scientific Research Grant Numbers 15J11371 and (C)15K06149.

REFERENCES

[1] P. Apkarian, P. Gahinet, and G. Becker, Self-Scheduled $\mathcal{H}_\infty$ Control of Linear Parameter-Varying Systems: A Design Example, *Automatica*, Vol. 31, No. 9, September (1995) 1251-1261.

[2] P. P. Khargonekar and M. A. Rotea, $\mathcal{H}_2/\mathcal{H}_\infty$ Control: A Convex Optimization Approach, *IEEE Transactions on Automatic Control*, Vol. 36, No. 7, (1991) 824-837.

[3] T. Shimomura and T. Kubotani, Gain-Scheduled Control under Common Lyapunov Functions: Conservatism Revisited, *Proc. of 2005 American Control Conference* (2005) 870-875.

[4] S. Di Gennaro, Passive Attitude Control of Flexible Spacecraft from Quaternion Measurements, *Journal of Optimization Theory and Applications*, Vol. 116, No. 1 (2003) 41-60.

[5] Q. Hu, Sliding Mode Maneuver Control and Active Vibration Damping of Three-axis Stabilized Flexible Spacecraft with Actuator Dynamics, *Nonlinear Dyn*, Vol. 52 (2008) 227-248.

[6] K. Enomoto, A Study on the Dynamic Inversion Method with Nonlinear Function Considering Saturation, *Proceedings of AIAA Guidance, Navigation, and Control Conference*, AIAA 2010-8205 (2010) Toronto, Canada.

[7] D. Ito, D. Ward and J. Valasek, Robust Dynamic Inversion Controller Design and Analysis for the X-38, *Proceedings of AIAA Guidance, Navigation, and Control Conference*, AIAA 2001-4380 (2001) Montreal, Canada.

[8] P. Cui and J. He, Steering Law for Two Parallel Variable-Speed Double-Gimbal Control Moment Gyros, *Journal of Guidance, Control, and Dynamics*, Vol. 37, No. 1, January-February (2014) 350-359.

[9] T. Sasaki and T. Shimomura, Fault-Tolerant Architecture of Two Parallel Double-Gimbal Variable-Speed Control Moment Gyros, *Proceedings of AIAA Guidance, Navigation, and Control Conference*, AIAA 2016-0090 (2016) San Diego, CA.

[10] B. Wie, D. Bailey and C. Heiberg, Singularity Robust Steering Logic for Redundant Single-Gimbal Control Moment Gyros, *Journal of Guidance, Control, and Dynamics*, Vol. 24, No. 5, September-October (2001) 865-872.

[11] P. W. Likins and G. E. Fleischer, Results of Flexible Spacecraft Attitude Control Studies Utilizing Hybrid Coordinates, *Journal of Spacecraft and Rockets*, Vol. 8, No. 3 (1971) 264-273.

[12] M. Sidi, Spacecraft Dynamics and Control, A Practical Engineering Approach, Cambridge Univ. Press, New York (1997) 241-242.

[13] C. E. Fossa, R. A. Raines, G. H. Gunsch and M. A. Temple, An Overview of the IRIDIUM Low Earth Orbit (LEO) Satellite System, *Proceedings of the IEEE National Aerospace and Electronics Conference, Inst. of Electrical and Electronics Engineers*, Piscataway, NJ (1998) 152-159.